

Pretraining with random noise for uncertainty calibration

Jeonghwan Cheon¹ and Se-Bum Paik^{1*}

¹Department of Brain and Cognitive Sciences, Korea Advanced Institute of Science and Technology, Daejeon 34141, Republic of Korea

* Correspondence author: sbpaik@kaist.ac.kr

Abstract

Uncertainty calibration, the process of aligning confidence with accuracy, is a hallmark of human intelligence. However, most machine learning models struggle to achieve this alignment, particularly when the training dataset is small relative to the network's capacity. Here, we demonstrate that uncertainty calibration can be effectively achieved through a pretraining method inspired by developmental neuroscience. Specifically, training with random noise before data training allows neural networks to calibrate their uncertainty, ensuring that confidence levels are aligned with actual accuracy. We show that randomly initialized, untrained networks tend to exhibit erroneously high confidence, but pretraining with random noise effectively calibrates these networks, bringing their confidence down to chance levels across input spaces. As a result, networks pretrained with random noise exhibit optimal calibration, with confidence closely aligned with accuracy throughout subsequent data training. These pre-calibrated networks also perform better at identifying "unknown data" by exhibiting lower confidence for out-of-distribution samples. Our findings provide a fundamental solution for uncertainty calibration in both in-distribution and out-of-distribution contexts.

One sentence summary

Pretraining with random noise enables networks to align confidence with accuracy, effectively calibrating uncertainty for both in-distribution and out-of-distribution data.

Research Highlights

- Deep neural networks often struggle to properly calibrate both accuracy and confidence.
- Pretraining with random noise aligns confidence levels with actual accuracy.
- Random noise pretraining facilitates meta-learning by aligning confidence with the chance level.
- Pre-calibrated networks assess both known and unknown datasets through confidence estimation.

Introduction

Recent advances in deep neural networks have significantly enhanced their ability to learn with accuracy¹. For instance, deep learning models achieved human-level accuracy in classifying natural images over a decade ago²⁻⁵. Building on this remarkable capability, deep neural networks are now being applied to a wide range of real-world problems that involve complex decision-making, such as autonomous driving systems^{6,7}, medical diagnosis^{8,9}, and financial engineering^{10,11}. However, in these applications, simply inferring the correct answer is insufficient; an additional dimension of information must be considered: confidence or uncertainty (Fig. 1). It is crucial to predict answers with calibrated probabilities that accurately reflect the likelihood of correctness.

Despite their remarkable capacity for accurate learning, modern deep neural networks are often poorly calibrated in terms of confidence estimation¹²⁻¹⁴. Specifically, the rapid increase in model capacity enables accurate classification but negatively impacts confidence calibration¹². Modern neural networks frequently exhibit overconfidence, even with out-of-distribution samples despite lacking knowledge about them^{15,16}. Miscalibrated confidence poses significant problems in real-world applications, where false predictions can be critical and costly¹⁷⁻²². Hallucinations in large language models²³⁻²⁶, where the model confidently produces false and unsubstantiated outputs²⁷⁻³⁰, are a well-known issue arising from the miscalibration of neural networks³¹⁻³³.

Several studies have proposed solutions to calibrate confidence for predictions from classifier models. These research efforts suggest post-processing techniques to compute calibrated probabilities from the naïve output of the trained network, such as binning the output probability^{12,34-36} or adjusting the level of network output^{12,36,37}. Recent studies also utilize Bayesian neural networks to achieve state-of-the-art performance in uncertainty calibration³⁸⁻⁴⁰, but they require computationally intensive repetitions to calculate uncertainty in each trial. Many state-of-the-art algorithms employ auxiliary networks or score functions to distinguish overconfident predictions for unseen out-of-distribution data from those for in-distribution data^{15,16,41-44}. Overall, previous research typically handles calibration issues separately for in-distribution data and unseen out-of-distribution data. Moreover, these methods often require

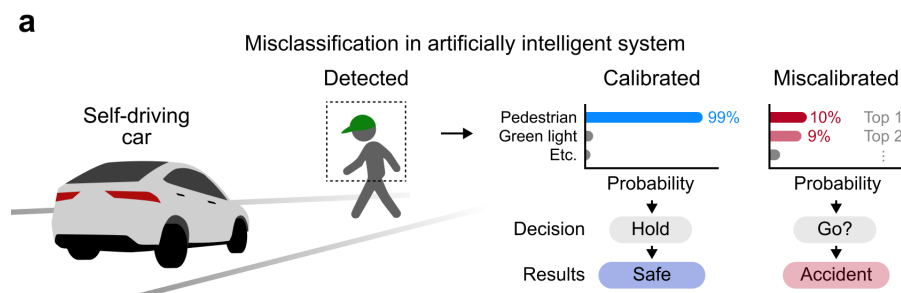


Fig. 1. Importance of uncertainty calibration in artificially intelligent systems

(a) The illustration depicts how self-driving cars detect objects in their environment and make decisions based on these detections. A pedestrian wearing a green cap is identified, and both the calibrated and miscalibrated models predict the same label. However, the confidence levels differ significantly between the two models. Miscalibrated confidence can lead to incorrect decisions, even when the predicted label is correct.

additional, computationally expensive steps to obtain calibrated confidence or auxiliary scores.

In contrast to the scenario in machine learning, where calibrated probabilities must be obtained through additional processes, human intelligence naturally exhibits meta-cognition, which estimates uncertainty and is aware of what is “known” and “unknown”⁴⁵⁻⁴⁸. This raises the question: what is the underlying mechanism of uncertainty calibration in the biological brain, and how can we enable artificial neural networks to learn human-like uncertainty calibration without relying on post-processing or auxiliary computation? To address this question, we draw inspiration from our previous work⁴⁹, which proposed pretraining with random noise as a method that mirrors the biological prenatal learning stage. Specifically, we focused on the fact that random noise pretraining stabilizes the input space to align with the output chance level uniformly before learning from data. We hypothesized that these initial calibrations could facilitate the learning of calibrated uncertainty during subsequent data training.

In this study, we demonstrate that pre-calibrating uncertainty through training with random noise enables neural networks to learn probabilities that accurately reflect the likelihood of correctness. Our findings show that randomly initialized neural networks tend to exhibit high confidence even when they lack sufficient knowledge, but training with random noise effectively reduces loss by calibrating this confidence to chance levels uniformly across input spaces. As a result, pre-calibrated networks learn calibrated probabilities with accuracy and confidence aligned throughout subsequent data training. Moreover, pre-calibrated networks exhibit lower confidence when encountering unknown data, aiding in the detection of out-of-distribution samples. Taken together, our results suggest pretraining with random noise as a simple yet powerful strategy to address uncertainty calibration issues.

Results

Failure of confidence calibration in deep neural networks

To investigate the issue of confidence calibration in deep neural network models, we used a feedforward neural network designed for pattern classification of three-channel natural images ($32 \times 32 \times 3$) into ten categories. The network consists of multiple hidden layers with ReLU nonlinearities and a final classification layer that employs the SoftMax function. For a given image sample, the model outputs probabilities for each object category (Fig. 2a), and the predicted label corresponds to the category with the maximum probability. The model also provides a measure of prediction confidence, which is derived from the probability assigned to the predicted category. The predictive uncertainty, can be quantified as the difference between the confidence value and one. Ideally, a neural network is expected to output calibrated confidence, where the confidence level accurately reflects the actual likelihood of the prediction being correct. In contrast, a poorly calibrated network may output confidence levels that do not correspond to the actual likelihood of correctness, leading to potential misinterpretations of the model's predictions.

We trained the feedforward neural network using a subset of the CIFAR-10 dataset⁵⁰, which consists of natural images labeled with ten classes representing animals and objects. After training, we evaluated the model's predictions and confidence using test images that were not part of the training set. Specifically, we investigated whether the

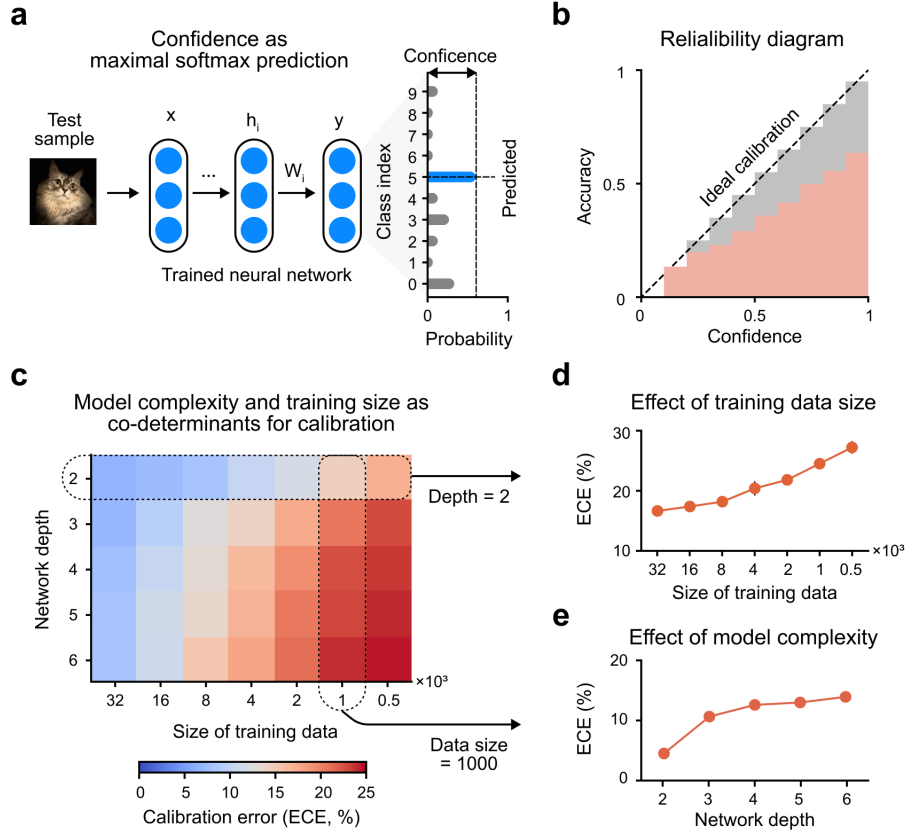


Fig. 2. Neural network complexity and data size as co-determinants for calibration

(a) The predicted answer and its confidence are calculated using the probability output from the SoftMax function. (b) Reliability diagram for a 2-layer feedforward neural network trained on a subset of the CIFAR-10 dataset (training data size = 1000). The test dataset's predictive confidence and correctness are binned based on confidence values, and the accuracy is calculated in each bin. The diagonal line represents ideal calibration, where the confidence perfectly matches the expected accuracy. The Expected Calibration Error (ECE) is the difference between predicted confidence and actual accuracy. (c) Calibration error across various model complexities and training data sizes. Each color represents the ECE: blue and red indicate low and high calibration error, respectively. (d) The effect of reducing the training data size on calibration error, with model complexity fixed (depth = 2). (e) The effect of increasing model complexity on calibration error, with training data size fixed (training data size = 1000).

confidence level of the trained network accurately reflects the likelihood of correctness. By measuring binned confidence values and the corresponding expected accuracy within each binned trial prediction, we constructed a reliability diagram^{37,51} to visualize the model's calibration (Fig. 2b). In this diagram, ideal calibration appears as an identity function, where the estimated confidence corresponds to the actual probability of correctness. In our results, we observed a significant gap between ideal calibration and the model's outputs. In general, the model's accuracy was lower than its confidence level, demonstrating the model's tendency for overconfidence.

We investigated the pattern of miscalibration by training neural networks of varying complexity with different training data sizes. To quantitatively measure the degree of miscalibration, we calculated the expected calibration error (ECE)⁵², which averages the difference between accuracy and confidence in each bin, weighted by the number of samples. As a result, we found that both model complexity and training data size systematically affect confidence

calibration (Fig. 2c). Specifically, we observed that the degree of miscalibration increases as the training data size decreases (Fig. 2d) and as model complexity increases (Fig. 2e). Thus, miscalibration arises when the training data is insufficient relative to the network’s complexity. This result explains why state-of-the-art models with high complexity struggle with the mismatch between confidence and accuracy. Recent network architectures often increase in structural depth to enhance learning capacity, but the available data size does not increase correspondingly. In real-world applications, acquiring and training on massive datasets is expensive and requires substantial computational resources. As a result, the miscalibration problem becomes inevitable in deep learning models.

Pretraining with random noise for confidence calibration

Recently, we introduced a novel strategy for pretraining networks inspired by the development of the biological brain⁴⁹. In this work, we demonstrated that pretraining networks with random noise enables robust learning without weight transport. Here, we revisit our random noise pretraining method and show that this process facilitates the preconditioning of networks, calibrating confidence to the chance level. We pretrained neural networks with noise inputs randomly sampled from a Gaussian distribution, and with random labels sampled from a uniform distribution (Fig. 3a, Supplementary Fig. 1). Notably, we observed that the loss gradually decreased when the network was trained with random noise, even though the accuracy remained at the chance level (Fig. 3b, Supplementary Fig. 2). Furthermore, when the network was trained with real data following the noise pretraining (Fig. 3b, Supplementary Fig. 3), we observed a more robust decrease in test loss during subsequent training, which was significantly lower than in networks trained without random noise pretraining (Fig. 3b). We also confirmed that the network pretrained with random noise achieved higher accuracy (Fig. 3c). These results demonstrate that pretraining with random noise enables faster and more effective loss reduction in subsequent training.

Next, we examined whether random noise pretraining can improve the calibration of probabilities to align confidence with accuracy levels. First, we measured the confidence distribution of the network’s output on the test dataset and compared it with the actual accuracy (Fig. 3d). We found that random noise pretraining significantly reduced the difference between confidence and accuracy in subsequent data training (Fig. 3e, w/o vs. w/ random pretraining, $n_{\text{net}} = 10$, Wilcoxon rank-sum test, $P < 10^{-3}$; w/o vs. zero, Wilcoxon signed-rank test, NS, $P < 10^{-3}$; w/ vs. zero, Wilcoxon signed-rank test, NS, $P = 0.131$). We also investigated the difference between the two networks using a reliability diagram (Fig. 3f). We observed that the randomly pretrained network’s outputs were closer to ideal calibration than those of networks trained with data alone. Additionally, we confirmed that the pretrained networks exhibited significantly lower calibration error compared to networks solely trained with data (Fig. 3g, w/o vs. w/ random pretraining, $n_{\text{net}} = 10$, Wilcoxon rank-sum test, $P < 10^{-3}$).

We then extended this analysis to neural networks trained with varying amounts of data and found that the effect of random noise pretraining in reducing calibration error was significant, regardless of the training data size (Fig. 3h, w/o vs. w/ random pretraining, $n_{\text{net}} = 10$, Wilcoxon rank-sum test, $P < 10^{-3}$). We also tested neural networks of different depths and confirmed the robust effect of noise pretraining (Fig. 3h, w/o vs. w/ random pretraining,

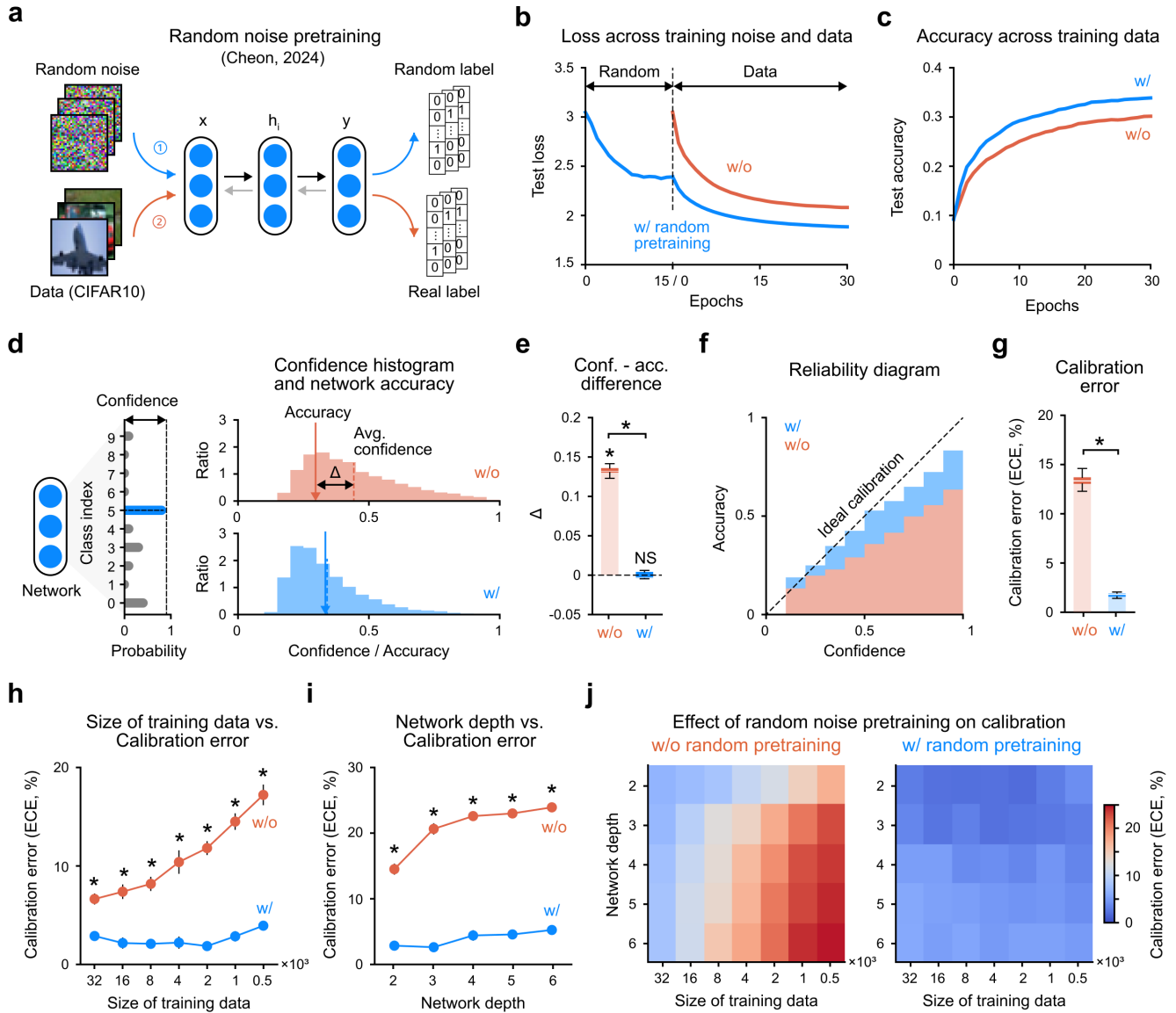


Fig. 3. Pretraining with random noise enables confidence calibration of neural networks

(a) Schematic illustrating the pretraining with random noise⁴⁹ and subsequent training with real data. During the random noise pretraining stage, the network is trained on randomly sampled inputs from a Gaussian distribution and randomly sampled labels from a uniform distribution, which are not paired. (b) Test loss across random noise pretraining and data training. The blue curve represents networks pretrained with random noise and subsequently trained with real data, while the orange curve represents networks trained solely with data. (c) Test accuracy during data training. (d) Histogram of confidence for a network trained only with data (orange) and a network pretrained with random noise (blue). Averaged accuracy and confidence are indicated by vertical lines. (e) The difference between averaged confidence and accuracy of predictions. (f) Reliability diagram showing the expected accuracy for samples binned by confidence. (g) Expected calibration error. (h) Effect of random noise pretraining on calibration error as training data size is reduced, with model complexity fixed (depth = 2). (i) Effect of random noise pretraining on calibration error as model complexity increases, with training data size fixed (training data size = 1000). (j) The combined effect of random noise pretraining under varying conditions of training data size and network complexity on calibration error.

$n_{\text{net}} = 10$, Wilcoxon rank-sum test, $P < 10^{-3}$). Furthermore, we measured calibration error for various combinations of training data size and network depth (Fig. 3j) and found that random noise pretraining successfully calibrated the confidence level across the conditions we examined. The effect of pretraining was particularly significant for networks with deep structures trained on smaller datasets, where confidence miscalibration typically occurs.

In addition to the current results using the standard training method with backpropagation, we also investigated neural networks trained with a biologically plausible algorithm, employing feedback alignment (Supplementary Fig. 4). We found that miscalibration also occurs in this type of model, suggesting that the issue of miscalibration is not limited to the backpropagation algorithm but may be a universal challenge across various algorithms. Notably, we observed that random noise pretraining significantly improves confidence calibration, even in this case, indicating that random noise pretraining could provide a general solution for confidence calibration across different models.

Pre-calibration of network uncertainty over input space via random noise

We further investigated how pretraining with random noise influences the properties of neural networks prior to their exposure to real data. To explore this, we introduced a simplified toy-model network with a two-dimensional input space (Fig. 4a), enabling straightforward visualization of the input space with only two features (Fig. 4b). Under these conditions, we observed that the initial state of a conventionally processed network — randomly initialized⁵³ and untrained — exhibited a highly biased and arbitrary distribution of confidence across the input space (Fig. 4b, Left). Additionally, we confirmed that this initial miscalibration was consistent across multiple trials with randomly initialized networks (Supplementary Fig. 5a).

In contrast, networks pretrained with random noise exhibited a more homogeneous distribution of confidence across the input space, effectively calibrated to the chance level (Fig. 4b, Right; Supplementary Fig. 5b). This result demonstrates that pretraining with random noise mitigates overconfidence by calibrating the confidence levels across the entire input space, bringing them closer to the chance level (Fig. 4c, w/ vs. w/o random pretraining, $n_{\text{trial}} = 1000$, Wilcoxon rank-sum test, $P < 10^{-3}$; Supplementary Fig. 5c). We also observed that untrained networks could exhibit initial biases toward specific output classes due to fluctuations in confidence. However, random noise pretraining significantly reduced this initial class bias, resulting in a more uniform confidence distribution across the classes (Fig. 4d, w/ vs. w/o random pretraining, $n_{\text{net}} = 10$, Wilcoxon rank-sum test, $P < 10^{-3}$).

Next, we extended this analysis to models with higher-dimensional input spaces (Fig. 4e). Specifically, the model used input features with dimensions of $32 \times 32 \times 3$ and output Softmax probabilities for ten classes, allowing it to train on CIFAR-10 data. We first measured the probability outputs for random noise inputs in both untrained and randomly pretrained networks (Fig. 4f). Consistent with the toy model results, we observed overconfidence and class bias in untrained networks (Fig. 4f, Left, $n_{\text{trial}} = 100$, one-way ANOVA, $P < 10^{-3}$), whereas such biases were barely detectable in randomly pretrained networks (Fig. 4f, Right, $n_{\text{trial}} = 100$, one-way ANOVA, NS, $P = 0.429$). We confirmed that the differences between the two networks were consistent with the toy model findings, both in the distribution of confidence (Fig. 4g, w/ vs. w/o random pretraining, $n_{\text{trial}} = 100$, Wilcoxon rank-sum test, $P < 10^{-3}$) and

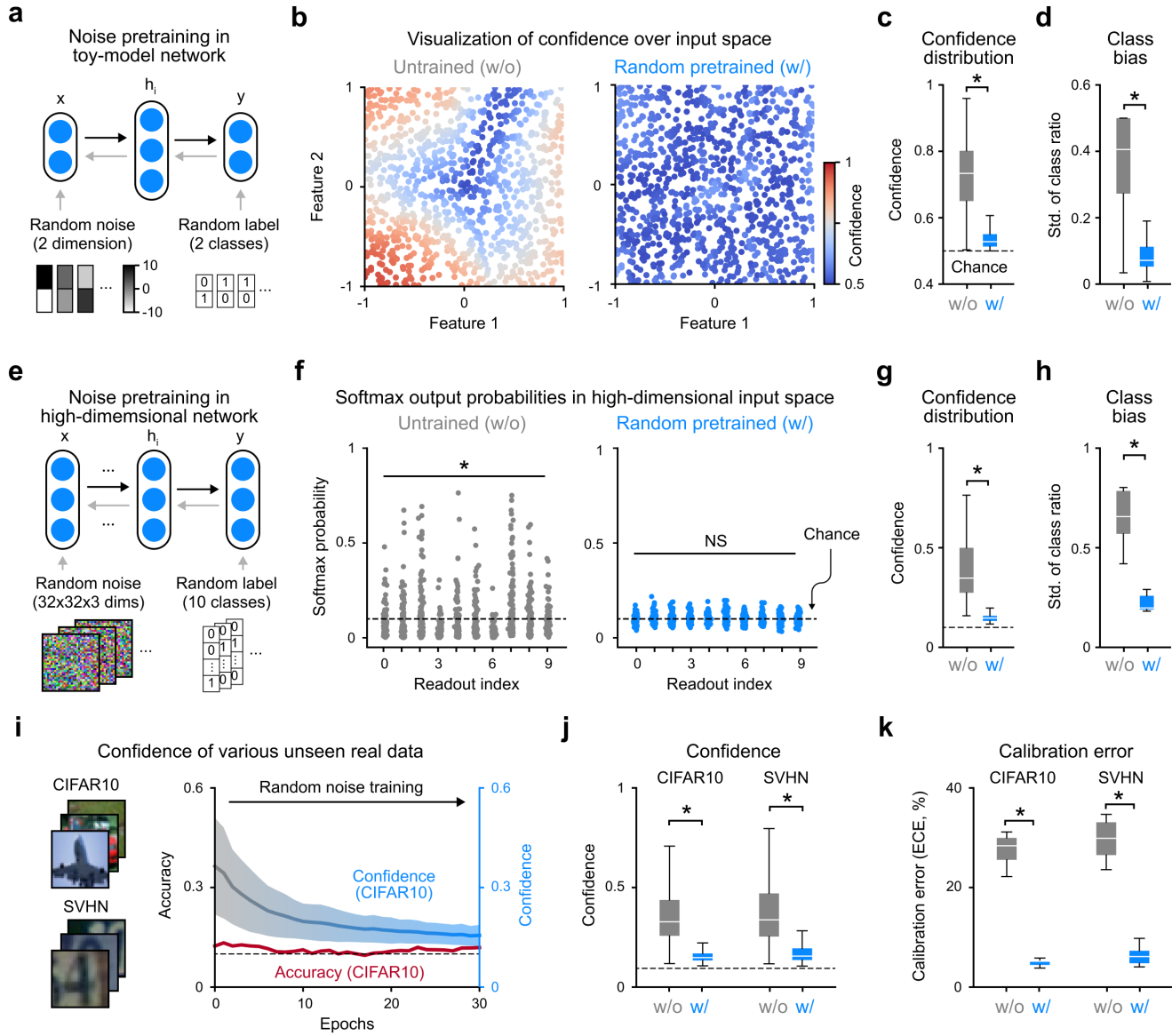


Fig. 4. Random noise pre-calibrates neural network uncertainty over input space

(a) Diagram illustrating the training of random noise in a toy-model network with a two-dimensional input space and binary output space. The network receives random noise with two input features and randomly assigned binary labels, and is trained using Binary Cross-Entropy (BCE) loss. (b) Visualization of confidence over the input space. (Left) Confidence map of the untrained network. (Right) Confidence map after random noise pretraining. (c) Confidence distribution of the network for two-dimensional noise. (d) Class bias of the network for two-dimensional noise, showing the extent of bias in class prediction. (e) Diagram of training random noise in a multi-layer perceptron with a high-dimensional input space, designed to classify the CIFAR-10 dataset. The network receives $32 \times 32 \times 3$ input images and outputs SoftMax probabilities for ten classes. (f) Visualization of SoftMax output probabilities for random noise inputs in the readout neurons. (Left) Untrained network. (Right) Network after random noise pretraining. The vertical line represents the chance level of classification. (g) Confidence distribution of the network for high-dimensional noise. (h) Class bias of the network for high-dimensional noise, showing the bias towards specific classes. (i-j) Confidence reduction for various unseen real data during random noise pretraining. (i) CIFAR-10 and SVHN datasets presented to the network during random noise training, with measured accuracy and confidence (Left). Confidence and accuracy for the CIFAR-10 dataset (Right). (j) Confidence distribution for CIFAR-10 and SVHN datasets before and after random noise pretraining. (k) Expected Calibration Error (ECE) for CIFAR-10 and SVHN datasets before and after random noise pretraining.

in class bias (Fig. 4h, w/ vs. w/o random pretraining, $n_{\text{net}} = 10$, Wilcoxon rank-sum test, $P < 10^{-3}$). These results suggest that random noise pretraining enables the network to maintain lower, more uniformly calibrated confidence levels, even when handling more complex, higher-dimensional input data.

We investigated whether the pre-calibration effect observed with random noise training extends to unseen, more realistic data. Specifically, we examined how the network’s confidence on CIFAR-10 and SVHN⁵⁴ datasets changes during random noise pretraining (Fig. 4i, Left) by measuring the network’s predictions for real data after each epoch during the pretraining phase. Initially, we observed that the confidence for unseen CIFAR-10 data was well-calibrated and approached the chance level, while accuracy remained at the chance level throughout random noise training (Fig. 4i, Right). We confirmed that this trend was consistent across different unseen datasets, including CIFAR-10 (Fig. 4j, CIFAR-10; w/ vs. w/o random pretraining, $n_{\text{trial}} = 10000$, Wilcoxon rank-sum test, $P < 10^{-3}$) and SVHN (Fig. 4j, SVHN; w/ vs. w/o random pretraining, $n_{\text{trial}} = 10000$, Wilcoxon rank-sum test, $P < 10^{-3}$). While accuracy remained at the chance level, the network maximized uncertainty for unseen data, aligning confidence with accuracy at the chance level. As a result, calibration error — the discrepancy between confidence and accuracy — was significantly reduced for unseen data (Fig. 4j, w/ vs. w/o random pretraining, $n_{\text{net}} = 10$, Wilcoxon rank-sum test, CIFAR-10, $P < 10^{-3}$; SVHN, $P < 10^{-3}$). These findings suggest that networks initialized conventionally tend to exhibit overconfidence and class bias even before training on data. In contrast, random noise pretraining effectively eliminates this initial bias and calibrates confidence to the chance level, maximizing uncertainty for unseen datasets. This result indicates that random noise pretraining can serve as a novel initialization strategy, offering an alternative to conventional random initialization⁵³.

Aligning confidence levels with actual accuracy during random noise pretraining

To further validate the effect of pre-calibration, we examined the learning dynamics of networks during subsequent training. To assess the impact of initial loss reduction — where the loss levels of networks were already lowered through random noise pretraining before learning from data — we investigated the training trajectory in a two-dimensional plane of accuracy and loss (Fig. 5a). Notably, the trajectory differed significantly between networks with and without random noise pretraining. Specifically, when comparing the points on both curves with the same accuracy value, we found that the randomly trained network had significantly lower loss values than the network trained solely on data. By selecting arbitrary points of the same accuracy (Fig. 5a, (1) and (2)), we examined the reliability diagram and calibration error for the two networks. We found that networks with random pretraining achieve better confidence calibration than those without pretraining, even with the same accuracy (Fig. 5b, w/o vs. w/ random pretraining, $n_{\text{net}} = 10$, Wilcoxon rank-sum test, $P < 10^{-3}$). Similarly, by selecting arbitrary points of the same total training epochs (Fig. 5a, (3), (4)), we observed that pretrained networks achieve better confidence calibration (Fig. 5c, w/o vs. w/ random pretraining, $n_{\text{net}} = 10$, Wilcoxon rank-sum test, $P < 10^{-3}$). These results demonstrate that random noise pretraining modulates the dynamics of subsequent learning, particularly by reducing the loss level for the same accuracy.

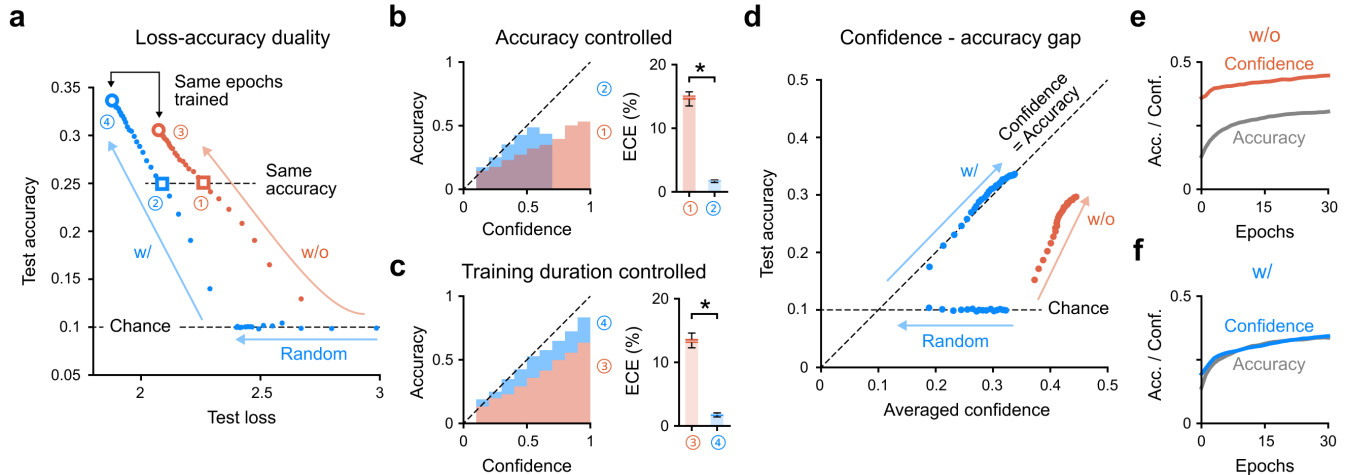


Fig. 5. Pre-calibration enables learning with matching confidence and accuracy

(a) Visualization of loss-accuracy duality. Each dot represents the test loss and accuracy at each epoch of training. Two points are selected for comparison of calibration: selected networks achieving the same accuracy for both the random noise pretrained network and the data-only training network (1, 2), as well as fully converged networks trained for the same number of epochs (3, 4). (b-c) Comparison between random noise pretrained networks and data-only training networks. (Left) Reliability diagram, showing the relationship between predicted confidence and accuracy. (Right) Calibration error, measured as Expected Calibration Error (ECE). (b) Accuracy-controlled comparison (1 vs. 2). (c) Epoch-controlled comparison (3 vs. 4). (d) Scatter plot of confidence versus accuracy for the training dataset in a data-only training network (orange) and a random noise pretrained network (blue). The diagonal line indicates perfect calibration, where confidence matches expected accuracy. (e-f) Averaged confidence and accuracy measured across training epochs for the training dataset. (e) Random noise pretrained network. (f) Data-only training network.

We next examined the relationship between confidence and accuracy throughout the entire training process, using a two-dimensional scatter plot of accuracy versus confidence (Fig. 5d). We found that in pretrained networks, confidence and accuracy were well-aligned, consistently lying near the diagonal line throughout training, while networks without pretraining did not exhibit this alignment (Fig. 5e). Specifically, a significant disparity between confidence and accuracy was initially observed due to early miscalibration, but this gap quickly diminished during random noise pretraining and ultimately disappeared. These initially aligned confidence and accuracy levels facilitate learning with synchronized confidence and accuracy during subsequent data training (Fig. 5f). Thus, calibrating confidence to the chance level through random noise pretraining before learning from data ensures proper calibration of predicted probabilities.

Detection of out-of-distribution samples using calibrated network confidence

Lastly, we investigated the effect of random noise pretraining on confidence calibration for out-of-distribution (OOD) data. OOD samples refer to unseen data that the model has not been trained on, in contrast to in-distribution (ID) samples, which the model has been trained on (Fig. 6a). After training our model on CIFAR-10 (ID), we measured the network's response to unseen SVHN data (OOD) (Fig. 6b). Notably, networks without random noise pretraining exhibited high confidence, even though they had no knowledge of OOD data (Fig. 6c, Left). In contrast, randomly pretrained networks showed significantly lower confidence for OOD samples, aligning closer to the chance level,

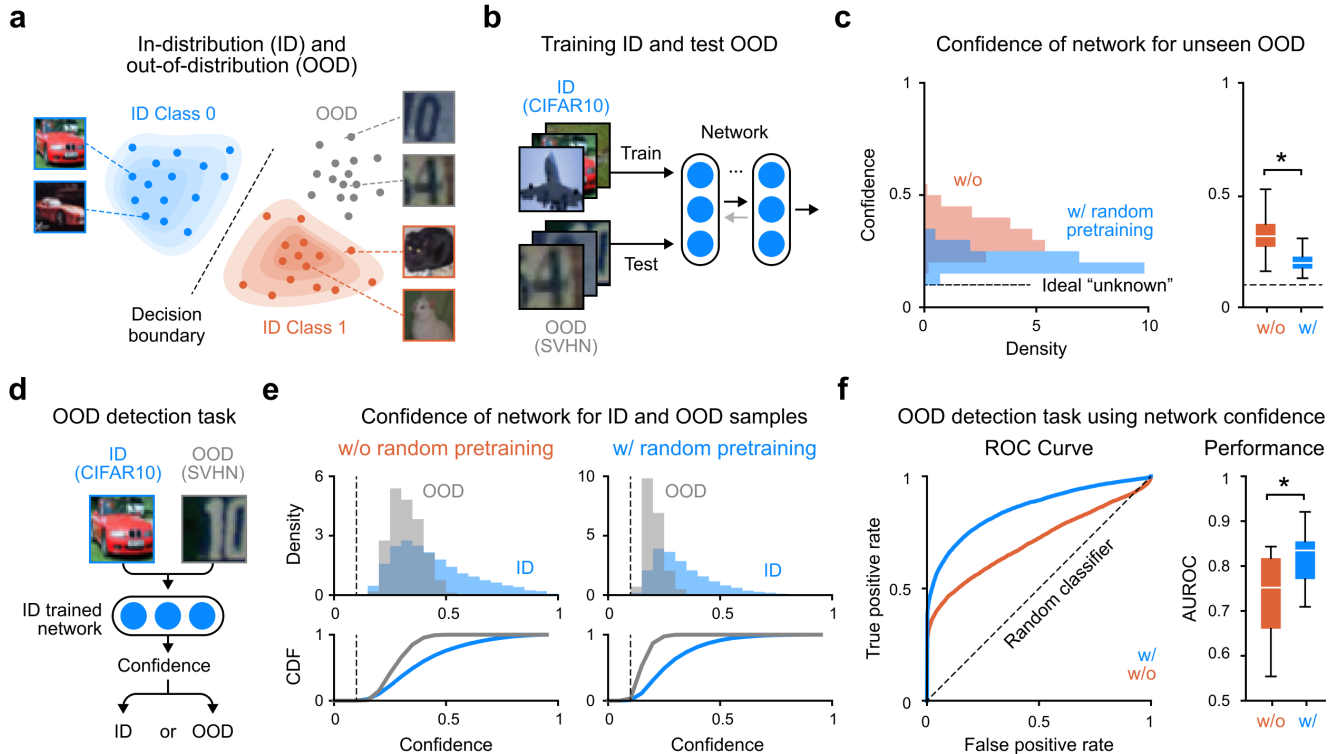


Fig. 6. Out-of-distribution detection using calibrated network confidence

(a) Conceptual illustration of In-Distribution (ID) and Out-Of-Distribution (OOD) samples. ID samples are those that the model has been trained on, while OOD samples are from a different distribution, not seen during training. (b) CIFAR-10 is used as ID data to train the neural network, and SVHN is used as OOD data, which the network has not been trained on. (c) Histogram of confidence for unseen OOD data (left). The distribution is also displayed as a boxplot (right). The horizontal line represents the chance level, indicating ideally calibrated confidence for unknown data, where the model exhibits maximized uncertainty. (d) Schematic of the OOD detection task. After training the network on ID data, both ID and OOD samples are presented to the network, and confidence is measured to determine whether the samples belong to the ID or OOD category. (e) Measured confidence for ID and OOD data and their Cumulative Distribution Functions (CDFs) in a data-only training network (left) and a random noise pretrained network (right). (f) Performance of the OOD detection task using network confidence. (Left) Receiver Operating Characteristic (ROC) curve, where the diagonal line represents random classification, and the point (0, 1) represents an ideal classifier. (Right) Performance of the OOD detection task, measured by the area under the ROC curve (AUROC).

which represents the ideal confidence for “unknown” data. We confirmed that randomly pretrained networks exhibited lower average confidence, closer to the chance level, for OOD samples (Fig. 6c, Right; w/ vs. w/o random pretraining, $n_{\text{Sample}} = 10000$, Wilcoxon rank-sum test, $P < 10^{-3}$).

We further investigated how calibrated confidence, for both in-distribution (ID) and out-of-distribution (OOD) samples, enhances the OOD detection task. To do this, we implemented a simple framework that used only raw confidence values to distinguish between ID and OOD samples (Fig. 6d). We analyzed the confidence histograms of ID and OOD samples and their cumulative distribution functions (Fig. 6e). In networks without pretraining, we observed significant overlap in the confidence histograms between ID and OOD samples, making it challenging to differentiate between the two groups (Fig. 6e, Left). In contrast, networks with random noise pretraining showed less

overlap, making the task easier (Fig. 6e, Right). We then measured the classification accuracy at various thresholds and plotted the results in the receiver operating characteristic (ROC) curve (Fig. 6f, Left). By calculating the area under the ROC curve (AUROC), we quantified the performance of the networks (Fig. 6f, Right). The results indicate that random noise pretraining significantly improves OOD detection performance (Fig. 6f, Right; w/ vs. w/o random pretraining, $n_{\text{net}} = 10$, Wilcoxon rank-sum test, $P < 10^{-3}$). These findings suggest that calibrated confidence helps maintain low confidence for unseen OOD data even after training with ID data. This implies that properly calibrated confidence, for both ID and OOD data, enables robust discrimination between "known" and "unknown" data without the need for post-processing or auxiliary computations.

Discussion

We demonstrated that pretraining with random noise enables neural networks to learn calibrated probabilities, aligning their confidence levels with expected accuracy. Specifically, we found that random noise training maximizes the initial uncertainty of the network's predictions, calibrating its confidence to the chance level. We validated that this pre-calibration allows networks to learn with reduced calibration errors. Furthermore, we showed that the network can effectively detect previously unseen data, i.e., out-of-distribution samples. These results suggest that properly calibrating the initial conditions through random noise training can significantly influence learning dynamics and enhance performance.

A longstanding question in machine learning concerns the proper initialization of neural networks for efficient learning. If the initialization is not appropriate, the network may converge to a local minimum or even diverge^{55,56}. Previous studies have shown that altering the initialization can help the network converge with higher accuracy^{53,57}. Several optimized initialization techniques have been proposed based on the network's activation function, which were considered optimal starting points for achieving higher accuracy. However, our results suggest that these previously proposed initialization methods are not ideal for learning in terms of calibration, as they tend to be initially overconfident and biased toward specific output neurons. We have confirmed that this initial miscalibration makes it challenging to align confidence with accuracy during subsequent training.

Previous research has primarily addressed overconfidence issues through post-calibration, where "calibrated confidence" is recalculated separately from the raw network output^{12,34-37}. In addition to post-calibration, recent studies have explored the potential of Bayesian neural networks to learn calibrated probabilities³⁸⁻⁴⁰. However, these methods require significantly more computational resources in addition to the original networks. Moreover, detecting out-of-distribution (OOD) samples necessitates auxiliary computations, such as training additional networks or calculating extra scores to identify unseen samples^{15,16,41-44}. Traditionally, the calibration of in-distribution (ID) and OOD samples has been treated as separate problems, often requiring additional, complex computations beyond the core learning process. In contrast, our proposed method offers a unified solution for both ID and OOD data, without the need for extra resources or post-processing.

While artificial intelligence struggles with calibration issues through post-calibration or auxiliary computations, human intelligence naturally exhibits meta-cognition — the ability to distinguish between what is known and what is unknown. Previous studies have demonstrated that humans possess an inherent ability to assess probabilistic confidence⁴⁷, and that estimating uncertainty plays a key role in complex human behaviors, particularly in decision-making^{45,46,48}. Our proposed method offers a straightforward solution to confidence calibration, enabling human-like uncertainty estimation and fostering meta-cognition. We anticipate that this approach will help address other challenging issues in machine learning caused by calibration, such as machine hallucination in large language models (LLMs).

Modern deep learning models are becoming increasingly complex to enhance their learning capacity. However, over-parameterization often results in miscalibration problems, as highlighted in previous research¹². We discovered that dataset size also plays a crucial role in calibration quality — when the dataset is insufficient, large and complex models experience significant calibration errors. This raises the question of whether an extremely large dataset is required to achieve optimal calibration as model complexity continues to increase. Our proposed method offers a solution by decoupling miscalibration issues from both dataset size and model complexity. This approach provides a simple yet effective strategy for modern deep neural networks as they evolve with more parameters.

We would like to emphasize that our work on pretraining with random noise is inspired by the prenatal developmental process of biological brains. Unlike artificial neural networks, which rely solely on training with real data, biological neural networks undergo preparatory learning before encountering sensory inputs from the external world. This preparation takes place through prenatal and spontaneous neural activity⁵⁸⁻⁶¹. Our recent work has shown that this random noise pretraining process, when combined with feedback alignment algorithms, offers a straightforward strategy that facilitates fast and robust learning without the need for weight transport⁴⁹. In the current study, our findings suggest that pretraining with random noise also enables human-like uncertainty calibration. This insight may offer a new perspective on the functional benefits of prenatal development in biological neural networks.

In summary, we conclude that pretraining with random noise effectively pre-calibrates network uncertainty, enabling subsequent learning with aligned accuracy and confidence. These results highlight the importance of the initial state of neural networks for effective data learning^{53,55,62-65}, as well as the significance of the early developmental process before encountering data^{49,66}. Our findings provide new insights into uncertainty calibration, offering potential solutions to challenges arising from calibration issues, such as machine hallucination.

Methods

Neural network model

We employed a multi-layer feedforward model as a simplified representative of conventional neural networks to investigate the miscalibration problem and the effect of random noise pretraining. The model consists of multiple non-linear layers, each performing a series of operations: multiplying weights, adding biases, and passing through a ReLU activation function. To mitigate overfitting, batch normalization was applied to every layer. The hidden layer size was fixed at 256 neurons, with the layer depth varied across different experiments. We observed that our results were fairly consistent regardless of hyperparameter settings, such as the hidden layer size, under typical conditions. The network weights were randomly initialized following a Gaussian distribution, with a mean of 0 and a standard deviation determined to control the gain across layers, as per the standard initialization method⁵³. The biases were initialized to zero.

Pretraining with random noise

The random noise input was sampled from a Gaussian distribution with a mean of 0 and a standard deviation of 1. We set the noise size to $32 \times 32 \times 3$, matching the size of the input data and the input dimension of the neural networks. The corresponding labels for the random noise were also randomly sampled from a uniform distribution and one-hot encoded. Both the random noise inputs and their labels were re-sampled at each iteration and were not paired with one another. During training, the random noise inputs were fed into the neural network, and the model output was obtained. The error was calculated as the distance between the model output and the random labels, and the network was trained to minimize this error, similar to conventional training procedures.

Subsequential training with real data

After pretraining the neural network with random noise, we proceeded to train it with real data. We used a subset of the CIFAR-10 dataset, which consists of $32 \times 32 \times 3$ natural images representing 10 categories: airplanes, automobiles, birds, cats, deer, dogs, frogs, horses, ships, and trucks. In the primary analysis, we used a training subset of 1000 samples to assess the robustness of calibration following random noise pretraining under challenging conditions. To investigate the effects of training data size and model capacity, we employed feedforward networks with depths of 2, 3, 4, 5, and 6 and trained them on CIFAR-10 subsets of sizes 500, 1000, 2000, 4000, 8000, 16000, and 32000.

For both the random noise pretraining and subsequent training with real data, we followed commonly used neural network training procedures. We applied standard backpropagation with the Adam optimizer, using learning rates between 0.0001 and 0.00001 and betas of (0.99, 0.999). To prevent overfitting, we used weight decay with a decay constant of 0.001. During the analysis, we compared the networks pretrained with random noise to those trained solely on data, without any random noise pretraining. All conditions, except for the random noise pretraining, were carefully controlled to isolate the effect of the random noise pretraining.

Additionally, we analyzed the neural network training using a feedback alignment algorithm, as a biologically plausible alternative to backpropagation that does not require weight transport. In feedback alignment, random synaptic feedback is used to compute the error signal, instead of using forward weights. Results obtained using this method are presented in the supplementary material.

Evaluating calibration of neural networks

To evaluate the calibration of the model, we used a reliability diagram, which visualizes the relationship between the model’s confidence and its actual accuracy. In this approach, we bin the model’s confidence and compute the expected accuracy within each bin. The reliability diagram then plots the expected accuracy as a function of the model’s confidence.

$$\text{acc}(B_m) = \frac{1}{B_m} \sum_{i=1}^{B_m} I(\text{pred}_i = \text{label}_i) \quad (1)$$

$$\text{conf}(B_m) = \frac{1}{B_m} \sum_{i=1}^{B_m} \text{conf}_i \quad (2)$$

, where M is the total number of bins, B_m is the number of samples in the m -th bin, N is the total number of samples, $\text{acc}(B_m)$ is the accuracy of the m -th bin, and $\text{conf}(B_m)$ is the average confidence in the m -th bin. In our simulations, we used 10 bins. To quantitatively measure the calibration of the model, we used the Expected Calibration Error (ECE), which calculates the average difference between the model’s confidence and its actual accuracy within the binned confidence. ECE is calculated as:

$$\text{ECE} = \sum_{m=1}^M \frac{B_m}{N} |\text{acc}(B_m) - \text{conf}(B_m)| \quad (3)$$

In an ideally calibrated model, the expected accuracy perfectly matches its confidence. Practically, a model is considered well-calibrated if its ECE is close to zero.

Visualization of confidence in toy-model and high-dimensional networks

As a proof-of-concept, we first employed a simple toy-model network with a two-dimensional (2D) input space. The input space is defined as the span of two features, each varying between -1 and 1. This allows us to visualize the input space in the 2D plane, where the x-axis represents the first feature and the y-axis represents the second feature. The neural network model consists of two layers, with a hidden layer of size 10. It outputs a two-dimensional vector for binary classification. The model is initialized using He initialization.

We trained this toy-model network with 2-dimensional random noise. Subsequently, we measured the model’s confidence for various inputs and plotted the resulting confidence on the input space, comparing both untrained and random-pretrained networks. This enables the visualization of the model’s confidence map across the input space. In addition, we analyzed the class bias of the model. The model outputs both the predicted class and its associated confidence. We calculated the ratio of predictions for each class and computed the standard deviation of these ratios:

$$\text{Class bias} = \text{std}([N_0, N_1, \dots, N_M] / \sum_{i=1}^M N_i) \quad (4)$$

where N_i represents the count of outputs predicted to class i , and M is the total number of output classes. A high class bias indicates that the model is biased toward specific readout neurons, while a class bias close to zero suggests that the model is unbiased, with predictions distributed more uniformly across the readout neurons.

To extend this analysis, we performed similar experiments with high-dimensional feedforward neural networks. We sampled high-dimensional random noise and measured the softmax probability output of the network. We visualized the model’s softmax outputs for both untrained networks and those pretrained with random noise. During the random noise pretraining of the high-dimensional networks, we also measured the confidence and accuracy for real data, such as CIFAR-10 and SVHN. Additionally, we calculated the expected calibration error (ECE) for CIFAR-10 and SVHN during random noise pretraining.

Out-of-distribution detection task

To design the out-of-distribution (OOD) detection task, we used CIFAR-10 as the in-distribution (ID) dataset for training. For the OOD samples, we selected SVHN, which also has a $32 \times 32 \times 3$ input size. After training the model on CIFAR-10, we measured the confidence of the network for both ID and OOD samples. Based on the measured confidence, we distinguished between ID and OOD samples by setting an arbitrary threshold. If the confidence exceeded the threshold, the sample was predicted as an ID sample; if the confidence was lower than the threshold, it was predicted as an OOD sample. Since the performance of OOD detection depends on the chosen threshold, we varied the threshold continuously from 0 to 1 and measured the corresponding false positive rate (FPR) and true positive rate (TPR). We then plotted the detection performance as a receiver operating characteristic (ROC) curve, with the true positive rate plotted against the false positive rate. To quantitatively assess the detection performance, we measured the area under the ROC curve (AUROC), which serves as a metric for the performance of OOD detection.

Statistical analysis

All statistical variables, including sample sizes, exact P values, and statistical methods, are provided in the corresponding text or figure legends.

Data availability

The datasets used in this study are publicly available: <https://www.cs.toronto.edu/~kriz/cifar.html> (CIFAR-10 and CIFAR-100), <http://ufldl.stanford.edu/housenumbers> (SVHN).

Code availability

The analysis and simulations were performed using Python 3.11 (Python software foundation) with PyTorch 2.1 and NumPy 1.26.0. Statistical tests were conducted using SciPy 1.11.4 was used to perform the statistical test and analysis. The code used in this study is available from the corresponding author upon request.

Acknowledgements

This work was supported by the National Research Foundation of Korea (NRF) grants (NRF2022R1A2C3008991 to S.P.) and by the Singularity Professor Research Project of KAIST (to S.P.).

Author contributions

J.C. conceived the project. J.C., and S.P. designed the model. J.C. performed the simulations. J.C. and S.P. analyzed the data. J.C. and S.P. wrote the manuscript and designed the figures.

Declaration of completing interests

The authors declare that they have no competing interests.

References

- [1] LeCun, Y., Bengio, Y. & Hinton, G. Deep learning. *Nature* **521**, 436–444 (2015).
- [2] LeCun, Y., Bottou, L., Bengio, Y. & Haffner, P. Gradient-based learning applied to document recognition. *Proceedings of the IEEE* **86**, 2278–2324 (1998).
- [3] Krizhevsky, A., Sutskever, I. & Hinton, G. E. Imagenet classification with deep convolutional neural networks. In Pereira, F., Burges, C., Bottou, L. & Weinberger, K. (eds.) *Advances in Neural Information Processing Systems*, vol. 25 (Curran Associates, Inc., 2012).
- [4] He, K., Zhang, X., Ren, S. & Sun, J. Deep residual learning for image recognition. In *Proceedings of the IEEE conference on computer vision and pattern recognition*, 770–778 (2016).
- [5] Huang, G., Liu, Z., Van Der Maaten, L. & Weinberger, K. Q. Densely connected convolutional networks. In *Proceedings of the IEEE conference on computer vision and pattern recognition*, 4700–4708 (2017).
- [6] Chen, Z. & Huang, X. End-to-end learning for lane keeping of self-driving cars. In *2017 IEEE intelligent vehicles symposium (IV)*, 1856–1860 (IEEE, 2017).
- [7] Yurtsever, E., Lambert, J., Carballo, A. & Takeda, K. A survey of autonomous driving: Common practices and emerging technologies. *IEEE access* **8**, 58443–58469 (2020).
- [8] Shen, D., Wu, G. & Suk, H.-I. Deep learning in medical image analysis. *Annual review of biomedical engineering* **19**, 221–248 (2017).
- [9] Litjens, G. *et al.* A survey on deep learning in medical image analysis. *Medical image analysis* **42**, 60–88 (2017).
- [10] Fischer, T. & Krauss, C. Deep learning with long short-term memory networks for financial market predictions. *European journal of operational research* **270**, 654–669 (2018).
- [11] Wei, H., Wang, Y., Mangu, L. & Decker, K. Model-based reinforcement learning for predictions and control for limit order books. *arXiv preprint arXiv:1910.03743* (2019).
- [12] Guo, C., Pleiss, G., Sun, Y. & Weinberger, K. Q. On calibration of modern neural networks. In *International conference on machine learning*, 1321–1330 (PMLR, 2017).
- [13] Minderer, M. *et al.* Revisiting the calibration of modern neural networks. In Ranzato, M., Beygelzimer, A., Dauphin, Y., Liang, P. & Vaughan, J. W. (eds.) *Advances in Neural Information Processing Systems*, vol. 34, 15682–15694 (Curran Associates, Inc., 2021).
- [14] Zhu, F., Cheng, Z., Zhang, X.-Y. & Liu, C.-L. Rethinking confidence calibration for failure prediction. In *European Conference on Computer Vision*, 518–536 (Springer, 2022).

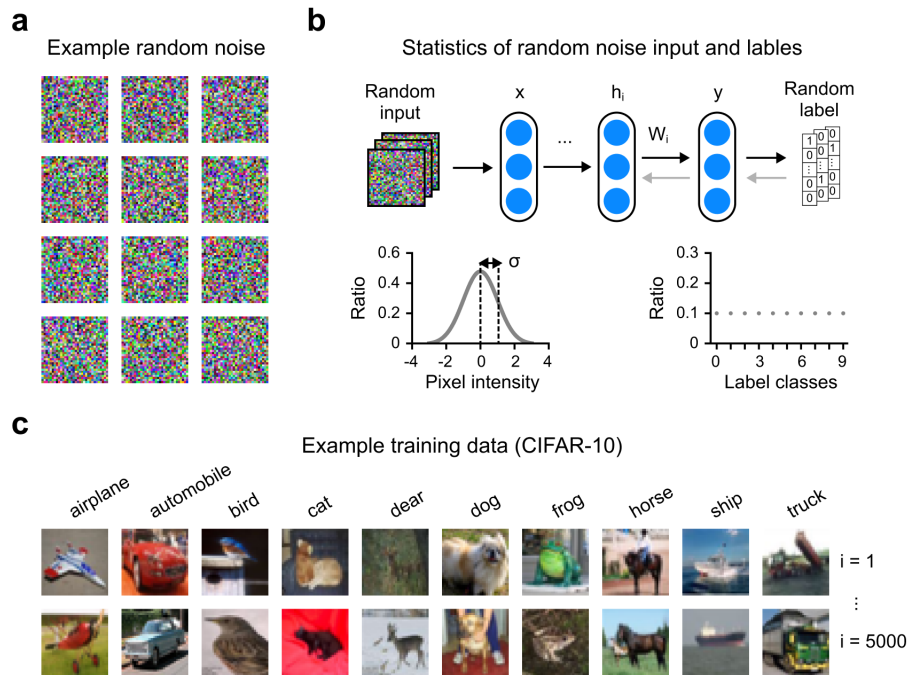
- [15] Hendrycks, D. & Gimpel, K. A baseline for detecting misclassified and out-of-distribution examples in neural networks. In *International Conference on Learning Representations* (2017).
- [16] Liang, S., Li, Y. & Srikant, R. Enhancing the reliability of out-of-distribution image detection in neural networks. In *International Conference on Learning Representations* (2018).
- [17] Mehrtash, A., Wells, W. M., Tempany, C. M., Abolmaesumi, P. & Kapur, T. Confidence calibration and predictive uncertainty estimation for deep medical image segmentation. *IEEE transactions on medical imaging* **39**, 3868–3878 (2020).
- [18] Jiang, X., Osl, M., Kim, J. & Ohno-Machado, L. Calibrating predictive model estimates to support personalized medicine. *Journal of the American Medical Informatics Association* **19**, 263–274 (2012).
- [19] Zwaan, L. & Hautz, W. E. Bridging the gap between uncertainty, confidence and diagnostic accuracy: calibration is key (2019).
- [20] Küppers, F., Haselhoff, A., Kronenberger, J. & Schneider, J. Confidence calibration for object detection and segmentation. In *Deep Neural Networks and Data for Automated Driving: Robustness, Uncertainty Quantification, and Insights Towards Safety*, 225–250 (Springer International Publishing Cham, 2022).
- [21] Helldin, T., Falkman, G., Riveiro, M. & Davidsson, S. Presenting system uncertainty in automotive uis for supporting trust calibration in autonomous driving. In *Proceedings of the 5th international conference on automotive user interfaces and interactive vehicular applications*, 210–217 (2013).
- [22] Michelmore, R. et al. Uncertainty quantification with statistical guarantees in end-to-end autonomous driving control. In *2020 IEEE international conference on robotics and automation (ICRA)*, 7344–7350 (IEEE, 2020).
- [23] Devlin, J., Chang, M.-W., Lee, K. & Toutanova, K. Bert: Pre-training of deep bidirectional transformers for language understanding. *arXiv preprint arXiv:1810.04805* (2018).
- [24] Achiam, J. et al. Gpt-4 technical report. *arXiv preprint arXiv:2303.08774* (2023).
- [25] Dubey, A. et al. The llama 3 herd of models. *arXiv preprint arXiv:2407.21783* (2024).
- [26] Team, G. et al. Gemini: a family of highly capable multimodal models. *arXiv preprint arXiv:2312.11805* (2023).
- [27] Farquhar, S., Kossen, J., Kuhn, L. & Gal, Y. Detecting hallucinations in large language models using semantic entropy. *Nature* **630**, 625–630 (2024).
- [28] Ji, Z. et al. Survey of hallucination in natural language generation. *ACM Computing Surveys* **55**, 1–38 (2023).
- [29] Xiao, Y. & Wang, W. Y. On hallucination and predictive uncertainty in conditional language generation. *arXiv preprint arXiv:2103.15025* (2021).

- [30] Rohrbach, A., Hendricks, L. A., Burns, K., Darrell, T. & Saenko, K. Object hallucination in image captioning. *arXiv preprint arXiv:1809.02156* (2018).
- [31] Groot, T. & Valdenegro-Toro, M. Overconfidence is key: Verbalized uncertainty evaluation in large language and vision-language models. *arXiv preprint arXiv:2405.02917* (2024).
- [32] Herlihy, C., Neville, J., Schnabel, T. & Swaminathan, A. On overcoming miscalibrated conversational priors in llm-based chatbots. *arXiv preprint arXiv:2406.01633* (2024).
- [33] Geng, J. *et al.* A survey of confidence estimation and calibration in large language models. In *Proceedings of the 2024 Conference of the North American Chapter of the Association for Computational Linguistics: Human Language Technologies (Volume 1: Long Papers)*, 6577–6595 (2024).
- [34] Zadrozny, B. & Elkan, C. Obtaining calibrated probability estimates from decision trees and naive bayesian classifiers. In *International Conference on Machine Learning*, vol. 18, 609–616 (2001).
- [35] Zadrozny, B. & Elkan, C. Transforming classifier scores into accurate multiclass probability estimates. In *Proceedings of the eighth ACM SIGKDD international conference on Knowledge discovery and data mining*, 694–699 (2002).
- [36] Platt, J. *et al.* Probabilistic outputs for support vector machines and comparisons to regularized likelihood methods. *Advances in large margin classifiers* **10**, 61–74 (1999).
- [37] Niculescu-Mizil, A. & Caruana, R. Predicting good probabilities with supervised learning. In *Proceedings of the 22nd international conference on Machine learning*, 625–632 (2005).
- [38] Blundell, C., Cornebise, J., Kavukcuoglu, K. & Wierstra, D. Weight uncertainty in neural network. In Bach, F. & Blei, D. (eds.) *Proceedings of the 32nd International Conference on Machine Learning*, vol. 37 of *Proceedings of Machine Learning Research*, 1613–1622 (PMLR, Lille, France, 2015).
- [39] Fortunato, M. *et al.* Noisy networks for exploration. In *International Conference on Learning Representations* (2018).
- [40] Gal, Y. & Ghahramani, Z. Dropout as a bayesian approximation: Representing model uncertainty in deep learning. In Balcan, M. F. & Weinberger, K. Q. (eds.) *Proceedings of The 33rd International Conference on Machine Learning*, vol. 48 of *Proceedings of Machine Learning Research*, 1050–1059 (PMLR, New York, New York, USA, 2016).
- [41] Hendrycks, D., Mazeika, M. & Dietterich, T. Deep anomaly detection with outlier exposure. In *International Conference on Learning Representations* (2019).
- [42] Lee, K., Lee, H., Lee, K. & Shin, J. Training confidence-calibrated classifiers for detecting out-of-distribution samples. In *International Conference on Learning Representations* (2018).

- [43] Lee, K., Lee, K., Lee, H. & Shin, J. A simple unified framework for detecting out-of-distribution samples and adversarial attacks. In Bengio, S. *et al.* (eds.) *Advances in Neural Information Processing Systems*, vol. 31 (Curran Associates, Inc., 2018).
- [44] Liu, W., Wang, X., Owens, J. & Li, Y. Energy-based out-of-distribution detection. In Larochelle, H., Ranzato, M., Hadsell, R., Balcan, M. & Lin, H. (eds.) *Advances in Neural Information Processing Systems*, vol. 33, 21464–21475 (Curran Associates, Inc., 2020).
- [45] Kepecs, A., Uchida, N., Zariwala, H. A. & Mainen, Z. F. Neural correlates, computation and behavioural impact of decision confidence. *Nature* **455**, 227–231 (2008).
- [46] Kiani, R. & Shadlen, M. N. Representation of confidence associated with a decision by neurons in the parietal cortex. *science* **324**, 759–764 (2009).
- [47] Cosmides, L. & Tooby, J. Are humans good intuitive statisticians after all? rethinking some conclusions from the literature on judgment under uncertainty. *cognition* **58**, 1–73 (1996).
- [48] Fleming, S. M. & Dolan, R. J. The neural basis of metacognitive ability. *Philosophical Transactions of the Royal Society B: Biological Sciences* **367**, 1338–1349 (2012).
- [49] Cheon, J., Lee, S. W. & Paik, S.-B. Pretraining with random noise for fast and robust learning without weight transport. In *Advances in Neural Information Processing Systems*, vol. 37 (2024).
- [50] Krizhevsky, A., Hinton, G. *et al.* Learning multiple layers of features from tiny images. Tech. Rep., University of Toronto (2009).
- [51] DeGroot, M. H. & Fienberg, S. E. The comparison and evaluation of forecasters. *Journal of the Royal Statistical Society: Series D (The Statistician)* **32**, 12–22 (1983).
- [52] Naeini, M. P., Cooper, G. & Hauskrecht, M. Obtaining well calibrated probabilities using bayesian binning. In *Proceedings of the AAAI conference on artificial intelligence*, vol. 29 (2015).
- [53] He, K., Zhang, X., Ren, S. & Sun, J. Delving deep into rectifiers: Surpassing human-level performance on imagenet classification. In *Proceedings of the IEEE international conference on computer vision*, 1026–1034 (2015).
- [54] Netzer, Y. *et al.* Reading digits in natural images with unsupervised feature learning. In *NIPS workshop on deep learning and unsupervised feature learning*, vol. 2, 4 (Granada, 2011).
- [55] Glorot, X. & Bengio, Y. Understanding the difficulty of training deep feedforward neural networks. In *Proceedings of the thirteenth international conference on artificial intelligence and statistics*, 249–256 (JMLR Workshop and Conference Proceedings, 2010).
- [56] Sutskever, I., Martens, J., Dahl, G. & Hinton, G. On the importance of initialization and momentum in deep learning. In *International conference on machine learning*, 1139–1147 (PMLR, 2013).

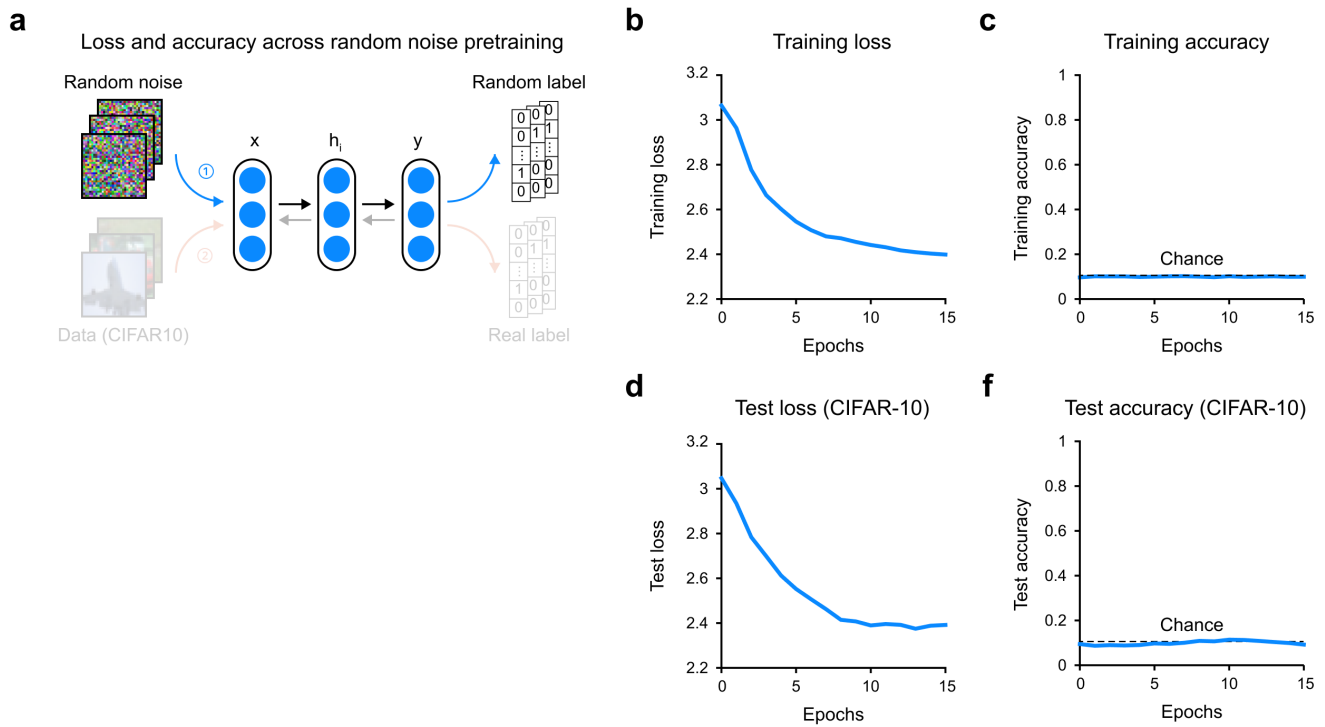
- [57] Saxe, A. M., McClelland, J. L. & Ganguli, S. Exact solutions to the nonlinear dynamics of learning in deep linear neural networks. *arXiv preprint arXiv:1312.6120* (2013).
- [58] Galli, L. & Maffei, L. Spontaneous impulse activity of rat retinal ganglion cells in prenatal life. *Science* **242**, 90–91 (1988).
- [59] Ackman, J. B., Burbridge, T. J. & Crair, M. C. Retinal waves coordinate patterned activity throughout the developing visual system. *Nature* **490**, 219–225 (2012).
- [60] Antón-Bolaños, N. *et al.* Prenatal activity from thalamic neurons governs the emergence of functional cortical maps in mice. *Science* **364**, 987–990 (2019).
- [61] Martini, F. J., Guillamón-Vivancos, T., Moreno-Juan, V., Valdeolmillos, M. & López-Bendito, G. Spontaneous activity in developing thalamic and cortical sensory networks. *Neuron* **109**, 2519–2534 (2021).
- [62] Kim, G., Jang, J., Baek, S., Song, M. & Paik, S.-B. Visual number sense in untrained deep neural networks. *Science advances* **7**, eabd6127 (2021).
- [63] Baek, S., Song, M., Jang, J., Kim, G. & Paik, S.-B. Face detection in untrained deep neural networks. *Nature communications* **12**, 7328 (2021).
- [64] Cheon, J., Baek, S. & Paik, S.-B. Invariance of object detection in untrained deep neural networks. *Frontiers in Computational Neuroscience* **16**, 1030707 (2022).
- [65] Lee, H., Choi, W., Lee, D. & Paik, S.-B. Comparison of visual quantities in untrained neural networks. *Cell Reports* **42** (2023).
- [66] Kim, J., Song, M., Jang, J. & Paik, S.-B. Spontaneous retinal waves can generate long-range horizontal connectivity in visual cortex. *Journal of Neuroscience* **40**, 6584–6599 (2020).
- [67] Rumelhart, D. E., Hinton, G. E. & Williams, R. J. Learning representations by back-propagating errors. *Nature* **323**, 533–536 (1986).
- [68] Lillicrap, T. P., Cownden, D., Tweed, D. B. & Akerman, C. J. Random synaptic feedback weights support error backpropagation for deep learning. *Nature communications* **7**, 13276 (2016).
- [69] Grossberg, S. Competitive learning: From interactive activation to adaptive resonance. *Cognitive science* **11**, 23–63 (1987).
- [70] Crick, F. The recent excitement about neural networks. *Nature* **337**, 129–132 (1989).

Supplementary Figures



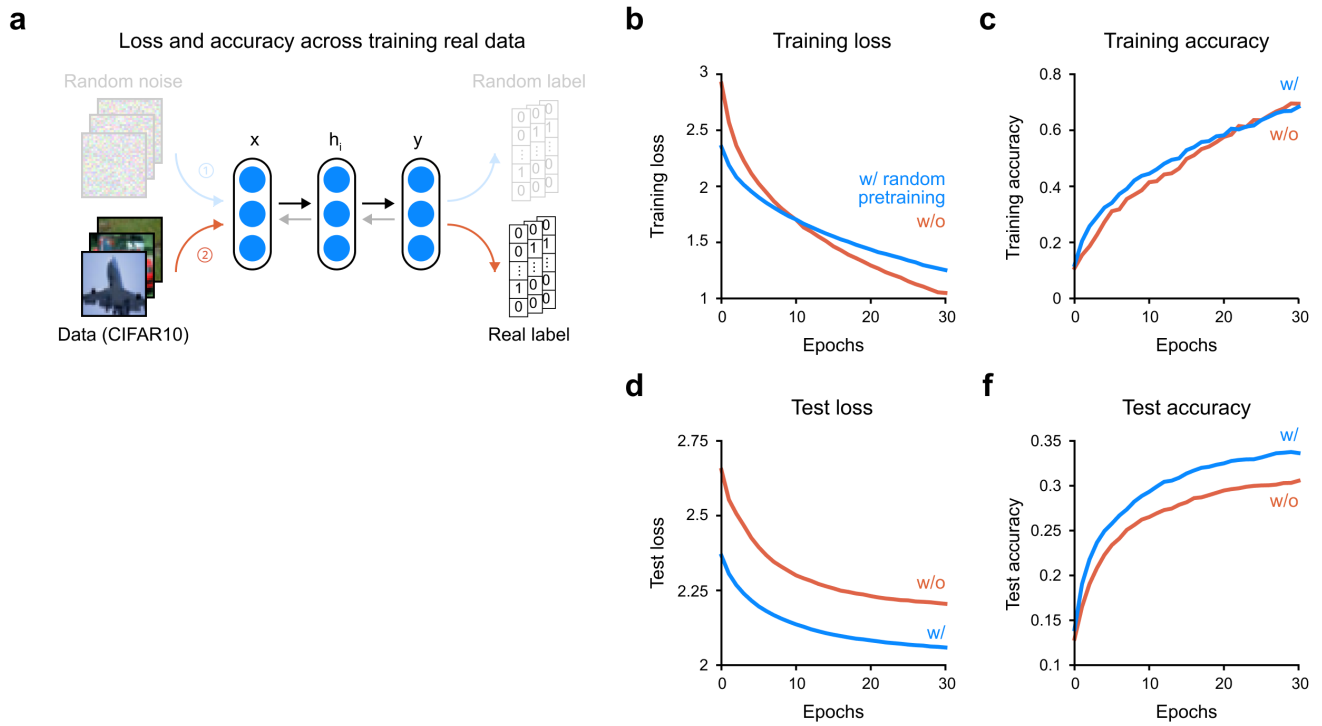
Supplementary Fig. 1. Random noise for pretraining and data for subsequent training

(a) Example of random noise ($32 \times 32 \times 3$) used in the pretraining phase of the network. This noise serves as an input during the initial random noise pretraining stage. (b) Statistics of the random noise and its corresponding random labels. The random noise is sampled from a Gaussian distribution with zero mean and a standard deviation of one. The random labels are sampled from a uniform distribution. In each iteration, random noise and labels are resampled and are not paired. (c) CIFAR-10⁵⁰, a benchmark natural image dataset used in the subsequent data training phase. CIFAR-10 consists of ten object and animal categories: Airplane, Automobile, Bird, Cat, Deer, Dog, Frog, Horse, Ship, and Truck.



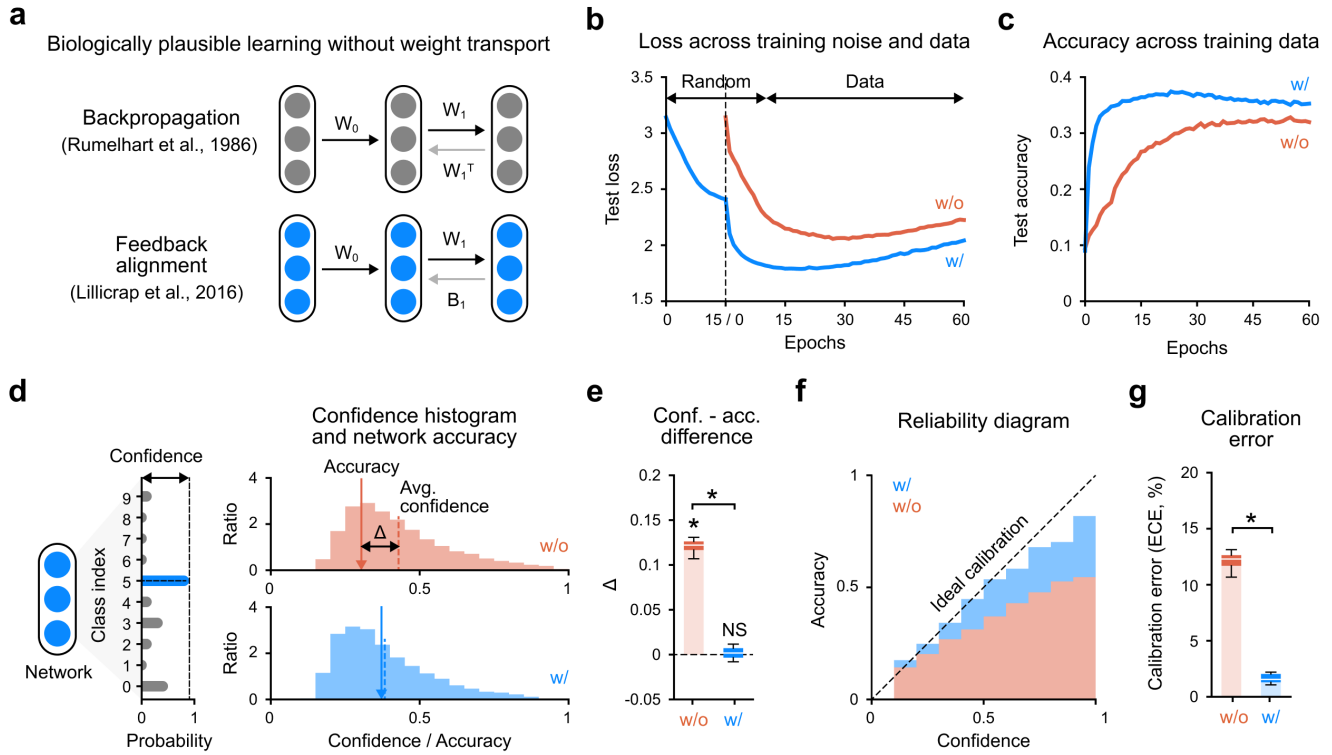
Supplementary Fig. 2. Learning curve in random noise pretraining

(a) The pretraining process, where neural networks are trained on random noise before encountering real data. (b-c) Learning curves during random noise pretraining: (b) Training loss (c) Training accuracy. Note that the accuracy remains at chance level, as there is no explicit correlation between the input (random noise) and the output labels.



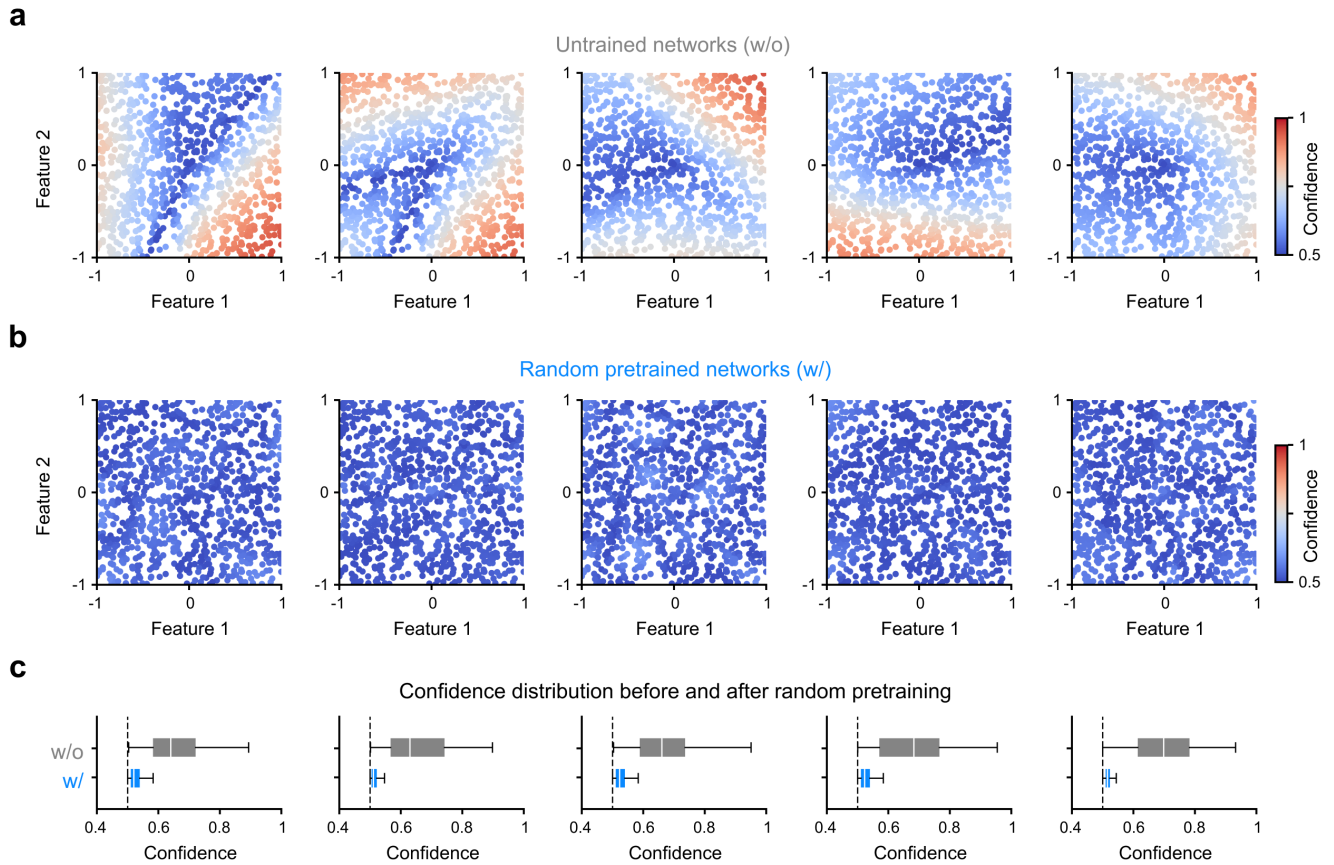
Supplementary Fig. 3. Learning curve in subsequent data training stage

(a) After pretraining with random noise, the network is subsequently trained with real data. (b-e) Learning curve during random noise pretraining. (b) Training loss. (c) Training accuracy. (d) Test loss. (e) Test accuracy. In each learning curve, the orange line represents the network trained solely with data (without random noise pretraining), while the blue line represents the network pretrained with random noise.



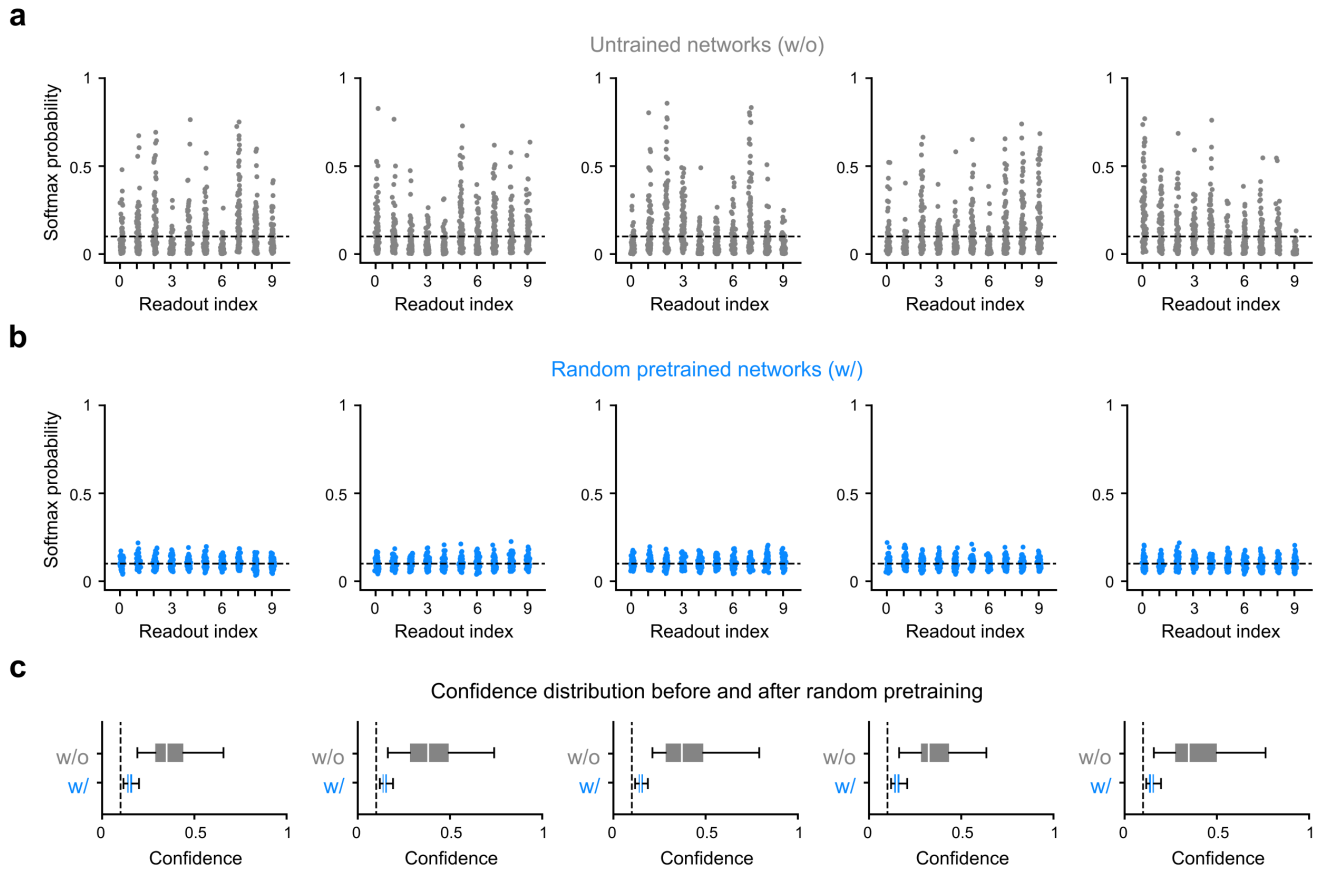
Supplementary Fig. 4. Uncertainty calibration via random noise pretraining with biologically plausible learning

(a) Comparison of backpropagation⁶⁷ and feedback alignment⁶⁸. Backpropagation is the standard training method for artificial neural networks but is not considered biologically plausible due to the weight transport problem^{69,70}, which requires a symmetric backward pathway for transmitting error signals. Feedback alignment, on the other hand, is a biologically plausible alternative that does not rely on weight transport, instead using a random matrix B to replace the backward synaptic pathway. (b) Test loss during random noise pretraining and subsequent data training. Blue indicates networks pretrained with random noise, and orange indicates networks trained solely with data (without random noise pretraining). (c) Test accuracy during subsequent data training. (d) Histogram of predictive confidence, with vertical lines indicating the averaged accuracy and confidence. (e) The difference between the averaged confidence and accuracy of predictions (w/o vs. w/ random pretraining, $n_{\text{net}} = 10$, Wilcoxon rank-sum test, $P < 10^{-3}$; w/o vs. zero, Wilcoxon signed-rank test, NS, $P < 10^{-3}$; w/ vs. zero, Wilcoxon signed-rank test, NS, $P = 0.752$). (f) Reliability diagram showing expected sample accuracy as a function of binned confidence. (g) Expected calibration error (w/o vs. w/ random pretraining, $n_{\text{net}} = 10$, Wilcoxon rank-sum test, $P < 10^{-3}$).



Supplementary Fig. 5. Pre-calibration of uncertainty in toy-model network

(a-c) To visualize the confidence over input space, a toy-model network with a two-dimensional input and output space was employed. Five trials with different random seeds were visualized. (a) Visualization of confidence over input space in the untrained network. (b) Visualization of confidence over input space in the random noise pretrained network. (c) Confidence distribution before and after random noise pretraining.



Supplementary Fig. 6. Pre-calibration of uncertainty in high-dimensional network

(a-c) A multi-layer feedforward neural network with a high-dimensional input space was employed to confirm uncertainty calibration via random noise pretraining. Five trials with different random seeds were visualized. (a) Visualization of SoftMax output probabilities in the untrained network. (b) Visualization of SoftMax output probabilities in the random noise pretrained network. (c) Confidence distribution before and after random noise pretraining.